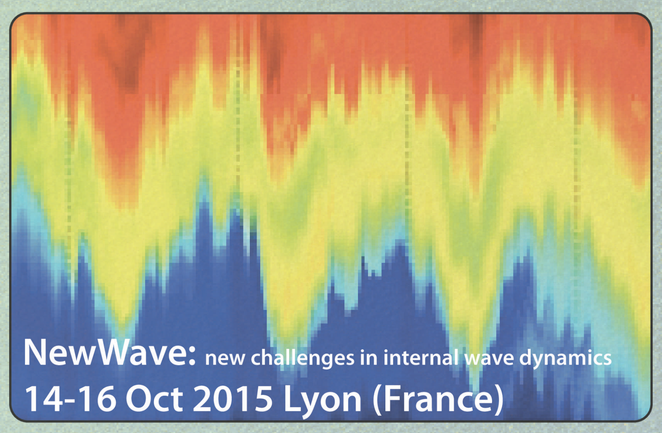

Large current systems and Internal Solitary Waves on and off the Amazon shelf as observed in SAR imagery

J.M. Magalhaes[1], J.C.B. da Silva[1], M.C. Buijsman[2], P. Calil[3], C.A.E. Garcia[3], J. Lorenzzetti[4], C. Macedo[4], C. Lentini[5], F. Pellon[6] de Miranda and C. Beisl[6]

1. Department of Geoscience, Environment and Spatial Planning, University of Porto, Porto, Portugal.
2. University of Southern Mississippi, Department of Marine Science, MS 39529, USA.
3. Federal University of Rio Grande, Institute of Oceanography, Rio Grande RS, Brazil.
4. INPE, Remote Sensing Division, São José dos Campos, São Paulo, Brazil.
5. Federal University of Bahia (UFBA), Dept. of Earth Physics and Environment, Salvador, Bahia, Brazil.
6. Petrobras, Petróleo Brasileiro S.A., Centro de Pesquisas e Desenvolvimento (CENPES), Rio de Janeiro, Brazil.

1-Intense Internal Solitary Waves off the Amazon Shelf

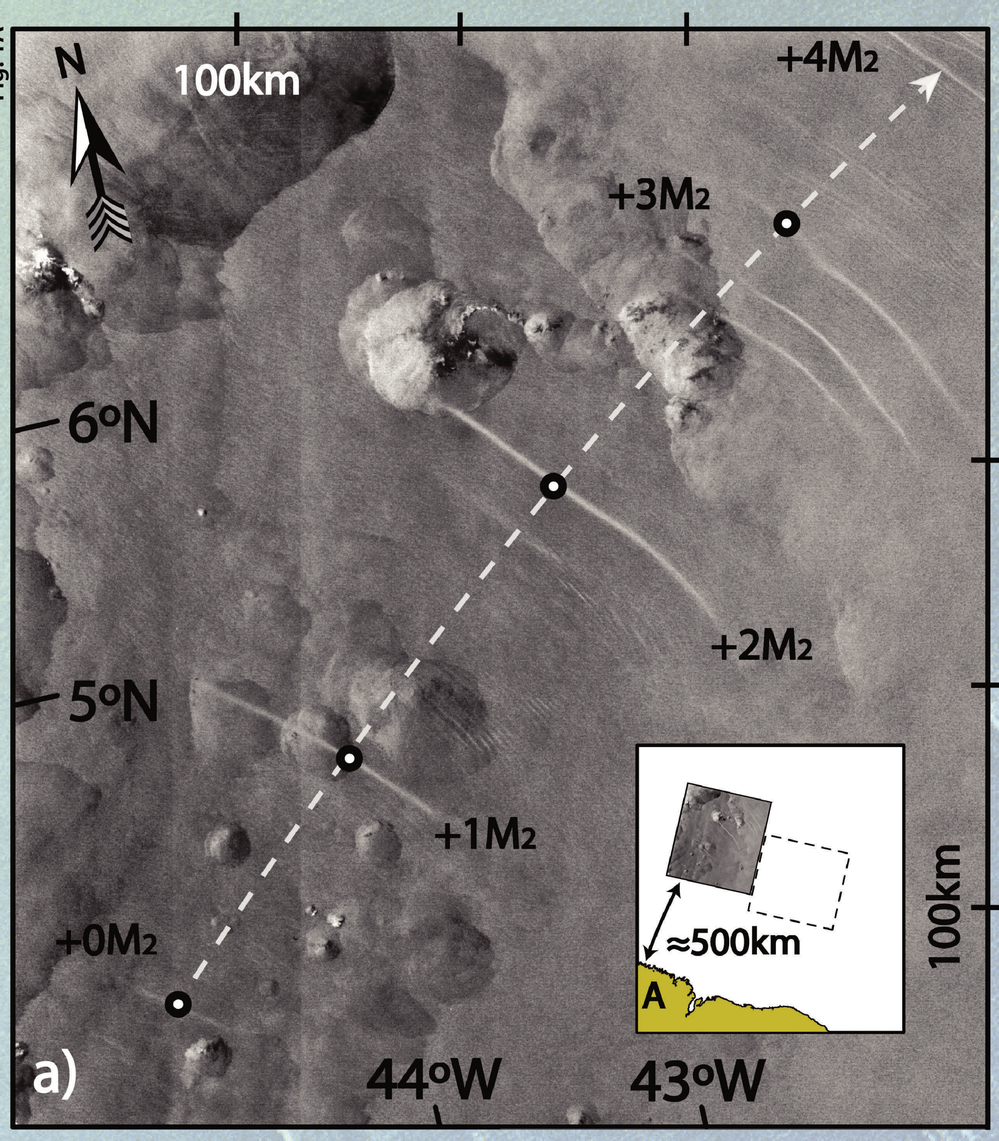

INTRODUCTION:

A significant amount of Internal Waves (**IW**) research is often motivated by satellite observations, which render their two-dimensional structure (see e.g. da Silva et al., 2015). In fact, newly unidentified hotspots, as well as previously studied regions, have been benefiting from satellite views, frequently providing new and deeper insights into their generation, propagation and dissipation mechanisms (e.g. Magalhaes and da Silva, 2012). While conveying their global character, synergetic views amongst different satellites, in situ and modelling data have also contributed to bridge this widespread phenomenon across multidisciplinary frameworks. Related fields of research currently span from the more fundamental oceanography to important applications in several oceanic and atmospheric fields, and open questions still remain concerning the global tide energy dissipation, in particular owing to IWs, which are important in ocean mixing and climate studies (Alford et al., 2015). A regained interest has also come from acknowledging IWs as one of the available mechanisms by which mass and momentum are transported in the oceans, and recognizing that sources and sinks may be significantly apart.

Fig. 1B

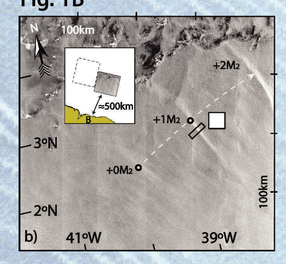

STUDY REGION:

The Amazon shelf-break is an important source for intense Internal Solitary Wave (**ISW**) observations and it is the focus of the present study (see e.g. Figs. 1A and 1B). It was early recognized in the work of Baines (1982) and is exceeded only by the Bay of Biscay and South China Sea. Similar results are equally found in recent models, which also rank this study region as a major hotspot in the conversion of barotropic to baroclinic energy (see e.g. Buijsman et al., 2015). The particular location of the Amazon shelf-break region adds further motivations to the oceanographic framework. It is placed in the tropical West Atlantic together with an intricate current system, including two major ocean currents – the North Equatorial Counter Current (**NECC**) and the North Brazilian Current (**NBC**, see Fig. 1C for locations). In turn, these are found very close to the Amazon River mouth, which accounts for roughly one third of the total fresh water input into the world's oceans (see e.g. Wisser et al., 2010).

SAR VIEWS:

Fig. 1C

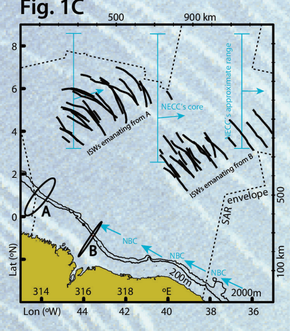

Satellite images acquired from Synthetic Aperture Radar (**SAR**) have proven very useful amongst other means of satellite remote sensing, which are typically used to survey ISWs, owing mainly to their extensive field of view along with detailed spatial resolution. Therefore, a representative dataset was assembled based on 17 SAR images, all of which belonging to the Envisat-ASAR and acquired in Wide-Swath mode. These span a period from 2004 to 2012 with no seasonal preferences being considered since favorable year round stratification conditions for ISWs are typical in these equatorial regions. Figs. 1A and 1B reveal the usual two-dimensional horizontal spatial structure of the ISW field and the characteristic sea surface signatures of intense ISWs appearing more than 500 km away from the nearest coastline (see insets and Fig. 1C for locations). Further inspection of the SAR signatures indicates multiple packets propagating offshore with a strong north-east component. The average inter-packet distances range from 121 to 140 km, which are typical wavelengths of long ITs of the fundamental mode (ISW packets have been labelled assuming consecutive semi-diurnal cycles). These average inter-packet distances can be converted into mean propagation speeds, since a semi-diurnal generation is being assumed. In this case the SAR images reveal these waves to be ranked amongst the fastest ever recorded with mean values ranging from 2.7 to 3.1 m/s (for locations B and A, respectively). There are two other interesting and somewhat unusual features in the SAR imagery concerning the typical view of the ISW field in this region. On the one hand, the wave packets usually consist of a few individual solitary waves, and on the other hand the ISW sea surface signatures are mostly given by very bright bands on a generally darker (i.e. greyish) background. The overall view of the entire dataset may be seen in Fig. 1C which presents a comprehensive view of the study region, together with a composite map for all SAR observations, whose envelope is shown by the black dashed line. For clarity, only the leading wave is depicted for each wavepacket (in black solid lines, with a total of 59 packets being represented). A well-organized ISW field can be seen running along two major pathways apparently associated with distinct hotspots, which have been labeled A and B close to the 200 m isobath, where representative tidal ellipses have be drawn from reference.

NECC:

Fig. 1D

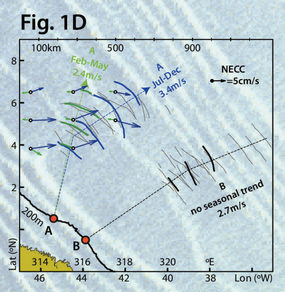

Fig. 1D highlights the seasonal differences in the dataset with two representative case studies corresponding to generation site A: one dated 27 May 2009 (in green), and another dated 3 October 2011 (in blue). It can be seen that, apart from being significantly refracted towards the east, the October ISWs show increased phase speeds (more than 30%), and seem to penetrate further into the open ocean. The seasonal character of the NECC is also depicted in the colored arrows marked along the waves' paths (in green and blue for May and October, respectively). The overall impression is that, between July and December (represented as the October data in blue) ISWs refract eastwards owing to the NECC, which acts not only to deflect the waves, but also provides an additional current in the along-ISW direction, contributing to their increased propagation speeds and ultimately to their extended penetration farther to the northeast. At the same time the other regime in the NECC (i.e. from February to May and represented as the May data in green) is quite the opposite. The NECC does not flow strongly to the east and refraction disappears as the currents weaken substantially during that period, to the point where currents reverse. Instead of contributing with an along-ISW current, the NECC changes direction so that currents now flow in the opposite direction, causing ISWs to decelerate along their propagation path.

GENERATION AND PROPAGATION DYNAMICS:

Despite the remote appearance of the ISW field (i.e. its unusually large distance from the shelf-break), its horizontal 2D spatial structure seen in Figs. 1A, 1B and 1C resembles that of the classical disintegration of an IT radiating from some forcing bathymetry, just as in many other hotspots like in the Bay of Biscay and the South China Sea. To further investigate the main generation characteristics of the IW field in the study region we now turn to modelling data corresponding to a series of simulations performed with the 3D global HYbrid Coordinate Ocean Model (HYCOM, see Bleck 2002 and Buijsman et al., 2015). Fig. 1E displays the depth integrated and time-mean conversion rates (left panel) and energy fluxes (right panel) for the semidiurnal tides, as is usually done to obtain a two-dimensional horizontal view of the IT generation field. The overall view seems to be consistent with the SAR data (i.e. composite map in black solid lines), since strong ITs appear to be generated over the steep slopes of the Amazon shelf, which then propagate along two major pathways into the open ocean. In fact, the strongest values in the left panel (i.e. concerning the conversion rates) are restricted to the shelf-break, and are seen running along the 200 m isobath, which decay rapidly either in the on-shore or off-shore directions. It is also important to stress that, local maxima are revealed along a small promontory (or headland – see reddish colors at locations A and B, near 44 °W and 0 °N) from which the ISWs appear to emanate, and where conversion values yield as high as 0.15 Wm^{-2}. This renders this region comparable to other known IT hotspots such as the Bay of Biscay and the South China Sea (see e.g. Buijsman et al., 2015). Finally, a significant decay may be found in between A and B, thus emphasizing the distinction between these two separate generation sites, where tidal ellipses are large and currents run mainly in the direction of the bathymetry gradient – therefore ideal for elevated conversion rates from the surface tide into the vertical baroclinic modes.

Depth-integrated energy fluxes (**FE** in Fig. 1E panel b) essentially convey where the IW energy is being held. According to these results, there are indeed two major pathways emanating from A and B, which contain the majority of the semidiurnal ITs and are in good agreement with the ISW directions depicted from the SAR data. However, it is interesting to see that ISWs are first seen as **FE** begins to decrease rapidly. This is likely a consequence of the filtered data (which shows only IWs at the semidiurnal frequency) or the larger spatial resolution of the HYCOM (around 8 km in this region). This means that the higher frequency ISWs may become undetectable in HYCOM filtered data. Therefore, a possible interpretation is that the IW energy is not simply being lost (e.g. as a result of dissipation), but also being transferred to the smaller-scale (and higher frequency) ISWs.

Fig. 1E

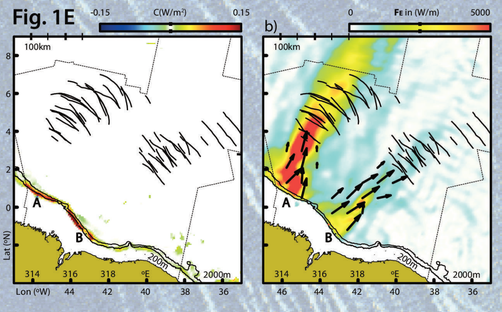

The generation of ITs is therefore consistent with the energetics analysis, and hence a likely possibility in the study region. However, it is yet to be explained why the ISW evidence is found much further than usual from their forcing bathymetry (i.e. the shelf-break), which in this case is more than several hundred km away into the open ocean (see Fig. 1C). We therefore proceed to some important considerations concerning the sequence of events leading to the evolution and disintegration of the IT. As described in Gerkema and Zimmerman (1995), the IT fate may be looked upon as an evolving process, where these large-scale waves will transform until balance between nonlinear and dispersive effects is eventually achieved. The sharp density front seen in Fig. 1F means that the thermocline's thickness (i.e the waveguide) will decrease when moving off-shore (corresponding to the green dashed line in Fig. 1D, using May climatological data from 1980 to 2011). The overall view is that the thermocline decreases more than 100 m between the shelf-break and the open ocean, as depicted by Ht which is taken to be between the bolded isopycnals - selected to be representative of the bulk of the thermocline.

Fig. 1F

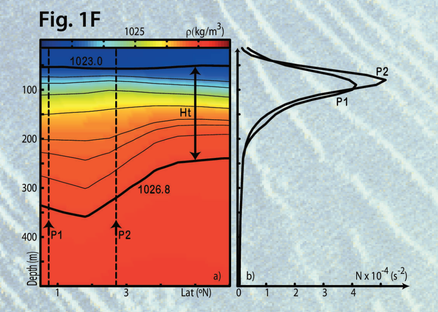

According to these results, the decrease in the thermocline seen in Fig. 1F forces the nonlinear parameter (Fig. 1G) to increase to higher values (green lines in panels a and b). Also shown in Fig. 1G is a disintegration envelope for the IT based on the numerical results presented in Helfrich and Grimshaw (2008). Note that in this case nonlinearity crosses this disintegration envelope precisely when the first ISWs appear in the SAR– i.e. between 3 and 4 °N (marked as transitions between solid and dashed lines). At the same time, changes in the thermocline vertical extension seem to be inconsequent to the nonhydrostatic dispersion seen in panel c, which is otherwise expected close to zero for the long wavelengths of the IT. The same applies to the rotational (or Coriolis) dispersion, but for different reasons, since it is the proximity to the equator that dictates the low values of μ. Altogether, this means that increasing nonlinearity (with no dispersion to compensate) will force the long IT to steepen and seek balance at the smaller wavelengths, up to the point where it may disintegrate into short-scale waves. During the course of disintegration the nonhydrostatic dispersion will increase quite substantially (since L drops by an order of magnitude) until balance may eventually lead to solitary-like waves.

Fig. 1G

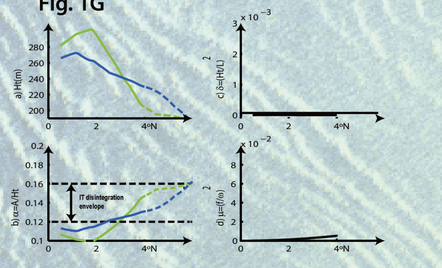

Check out more at:
http://jmagalhaes.wix.com/internal-waves-

2-Intense Internal Solitary Waves on the Amazon Shelf

Fig. 2A

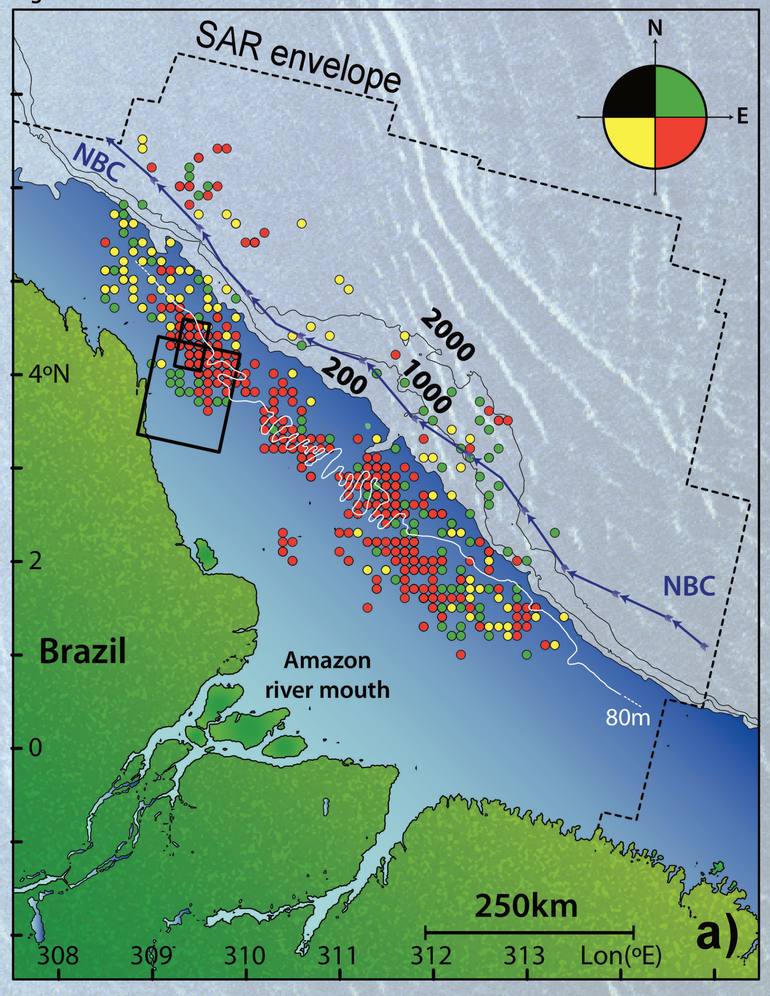

Fig. 2B

Fig. 2C

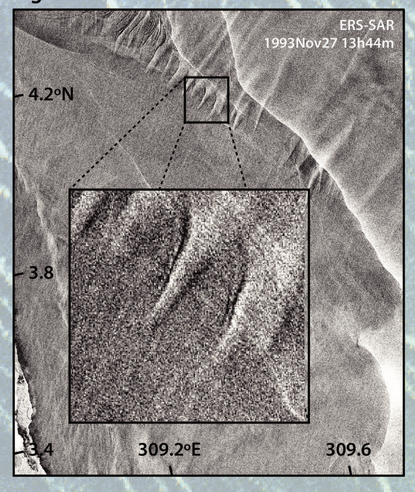

NEW SAR OBSERVATIONS - A PRELIMINARY ACCOUNT:

A new SAR dataset has been recently collected over the Amazon shelf, gathering multiple SAR missions (ERS, Envisat, Radarsat and TerraSAR-X) and several tens of images. A composite map is shown in Fig. 2A with all ISW packet observations being marked as a coloured dots according to their apparent direction of observation (see inset in top right corner). The overall impression from the SAR imagery is a well-spread ISW field raging along mid-shelf and generally propagating to the southeast against the North Brazilian Current (NBC). A typical view of the ISW field is shown in detail in Fig. 2B (its corresponding location is shown in the black rectangle in Fig. 2A) and reveals a series of well-defined wave packets separated by distances around 5 km, and propagating in water depths of approximately 80 m. These characteristic inter-packet separations do not fit the standard semi-diurnal tidally generated ISWs usually seen propagating over the shelf and hence are probably associated with a different generation mechanism.

A different hypothesis could be related to the intricate shallow bottom topography running along the mid-shelf region at the waves' locations (see Fig. 1A and the 80m isobath in white). In fact, having a strong current (NCB typically amounts to 1m/s) running in the opposite direction could favour a critical regime since such shallow depths usually dictate intrinsic phase speeds of that same order of magnitude. Quite interestingly, shallow bottom features may be imaged in SAR if the right conditions are set, and that appears to be exactly the case in Fig. 2C whose location (see black square, Fig. 2A) is partially coicident with that from Fig. 2B. Indeed a series of bottom features seem to be running very closely to the waves.

Furthermore, a zoom on some of these bottom features seems to reveal the very early stages of wave formation, where wave-like patters appear coincidently with the SAR signatures of bottom bathymetry (see inset in Fig. 2C). To further clarify this possibility both images have been overlaid in the same geographic frame in Fig. 2D. Apart from very similar spatial scales between both features (i.e. bottom and wave signatures), a rather conspicuous match seems to emerge at the boundary between both images. Critical flow may than be at the source of these observations and hence a careful analysis is currently being conducted based on the Froude number and the local thermodynamic conditions (i.e. stratification and currents) to challenge or confirm this hypothesis.

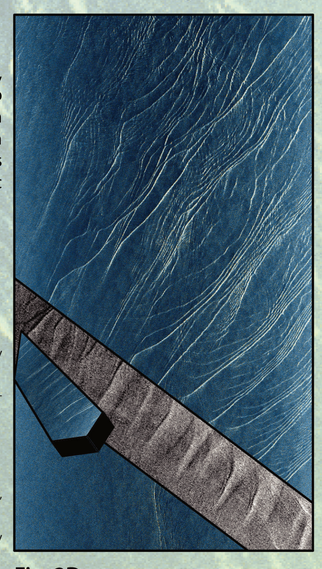

Fig. 2D

IMPORTANT REFERENCES:

Alford, M.H., Peacock, T., MacKinnon, et al., **2015**. The formation and fate of internal waves in the South China Sea. Nature 521, 65–69. doi:10.1038/nature14399.

Baines, P.G., **1982**. On internal tides generation models. Deep-Sea Res. Part A 29, 307–338, doi:http://dx.doi.org/10.1016/0198-0149(82)90098-X.

Bleck, R., **2002**. An oceanic general circulation model framed in hybrid isopycnic Cartesian coordinates. Ocean Modell. 4, 55–88. doi:10.1016/S1463-5003(01)00012-9.

Buijsman, M.C., Ansong, J.K., Arbic., B.K., Richman, J.G., Shriver, J.F., Timko, P.G., Wallcraft, A.J., Whalen, C.B., Zhao, Z., **2015**. Impact of internal wave drag on the semidiurnal energy balance in a global ocean circulation model. In Revision in Journal of Physical Oceanography.

da Silva, J.C.B., Buijsman, M.C., Magalhaes, J.M., **2015**. Internal waves on the upstream side of a large sill of the Mascarene Ridge: a comprehensive view of their generation mechanisms. Deep-Sea Res. I 99, 87-104. doi:10.1016/j.dsr.2015.01.002.

Gerkema, T., Zimmerman, J.T.F., **1995**. Generation of Nonlinear Internal Tides and Solitary Waves. J. Phys. Oceanogr. 25, 1081–1094.

Helfrich, K.R., Grimshaw, R.H.J., **2008**. Nonlinear Disintegration of the Internal Tide. J. Phys. Oceanogr. 28, 686–701. doi:10.1175/2007JPO3826.1.

Magalhaes, J.M., da Silva, J.C.B., **2012**. SAR observations of internal solitary waves generated at the Estremadura Promontory off the west Iberian coast, Deep Sea Res., Part I, 69, 12–24, doi:10.1016/j.dsr.2012.06.002.

Winner, D., Fekete, B.M., Vörösmarty, C.J., Schumann, A.H., **2010**. Reconstructing 20th century global hydrography: a contribution to the Global Terrestrial Network-Hydrology (GTN-H). Hydrol. Earth Syst. Sci, 14, 1–24. doi:10.5194/hess-14-1-2010.